Structural Engineering and Mechanics, *Vol. 71, No. 3 (2019) 271-282*
DOI: https://doi.org/10.12989/sem.2019.71.3.271

Span limit and parametric analysis of cable-stayed bridges

Xinwei Zhao, Rucheng Xiao and Bin Sun*

Department of Bridge Engineering, Tongji University, 1239 Siping Rd., Shanghai 200092, China

(Received November 8, 2018, Revised March 18, 2019, Accepted April 2, 2019)

Abstract. The span record of cable-stayed bridges has exceeded 1,000 m, which makes research on the maximum possible span length of cable-stayed bridges an important topic in the engineering community. In this paper, span limit is discussed from two perspectives: the theoretical span limit determined by the strength-to-density ratio of the cable and girder, and the engineering span limit, which depends not only on the strength-to-density ratio of materials but also on the actual loading conditions. Closed form equations of both theoretical and engineering span limits of cable-stayed bridges determined by the cable and girder are derived and a detailed parametric analysis is conducted to assess the engineering span limit under current technical conditions. The results show that the engineering span limit of cable-stayed bridges is about 2,200 m based on materials used available today. The girder is the critical member restricting further increase in the span length; its compressive stress is the limiting factor. Approaches to increasing the engineering span limit are also presented based on the analysis results.

Keywords: cable-stayed bridge; span limit; cable sag; strength-to-density ratio; height-to-span ratio; sagging cable efficiency

1. Introduction

The applicable span of early modern cable-stayed bridges ranged from 200 to 550 m. Advancements in engineering materials, computational theory, and construction methods, as well as increased demand for longer bridge spans, have driven the span of today's cable-stayed bridges well above this range (Virlogeux 1999). The Stromsund Bridge (Sweden), with a main span of 183 m, was opened to traffic in 1956; by 2012, the Russky Bridge (Russia) was completed with a main span length of 1,104 m (Fig. 1). In just over half a century, the span of cable-stayed bridges has increased more than five-fold while the span of suspension bridges has only increased by 55% (Gimsing 2005).

After the span of cable-stayed bridges broke 1,000 m, modern bridge engineers became confident that the span of cable-stayed bridges could be continually further increased. In the past 30 years, international bridge experts have extensively researched super-long span cable-stayed bridges. Leonhardt and Zeller (1991), for example, proposed an 1,800 m span conceptual design. Japanese experts proposed the Honshu-Shikoku 1,400 m span cable-stayed bridge (Nagai *et al*. 2004). Chinese experts investigated the feasibility of developing 2,000 m span cable-stayed bridges based on the Sutong Bridge (Cao *et al*. 2009) and 1,500 m multi-span cable-stayed bridges as replacements for suspension bridge anchorages in deep water (Tang 2014). These and other valuable contributions to the literature raise several questions: to what length can the span of cable-stayed bridges be theoretically increased based on the materials used today? What is the possible limit and which factors determine this limit?

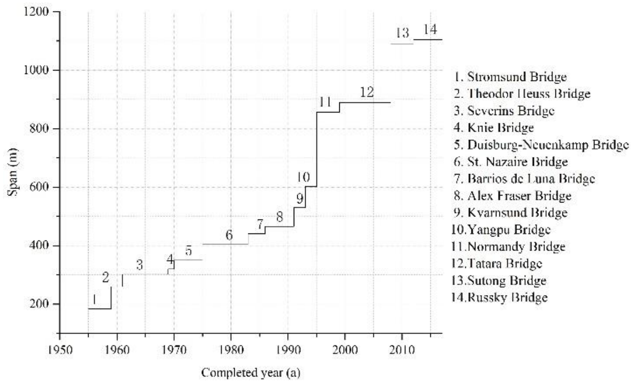

Fig. 1 Span evolution in modern cable-stayed bridges

Many researchers have studied the span limit of cable-stayed bridges differently based on the assumption that the limiting factor in the bridge span is the allowable stress through analytical methods. Wu (1996), Wang (2002), Lewis (2012), Zhang (2013), and Tang (2017) considered the maximum possible span length of a steel cable-stayed bridge to be about 2,900 m, 1,820 m, 7,000 m, 2,250 m, and 5,200 m, respectively. Their theoretical analysis models, however, contained oversimplified and impractical assumptions such as ignoring the cable sag, representing the cables as an equivalent cable "curtain", keeping the girder's cross-section constant, considering the limiting length determined by a non-load carrying cable, and regarding a stay cable of reasonable length as a part of a stay cable with the theoretical limiting length. Moreover, the effect of continuous cable distribution and different types of cable system were not taken into account in most studies on the maximum span length determined by the girder due to

*Corresponding author, Associate Professor
E-mail: sunbin@tongji.edu.cn

http://www.techno-press.com/journals/sem&subpage=7

ISSN: 1225-4568 (Print), 1598-6217 (Online)

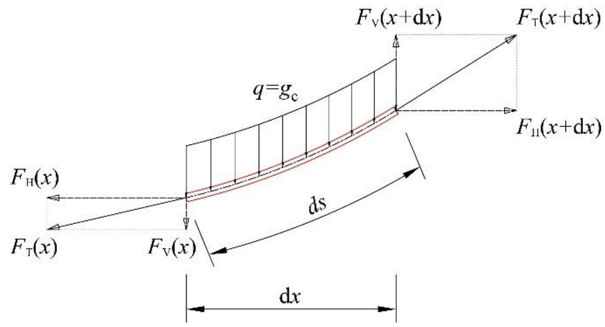

Fig. 2 Force diagram of infinitesimal cable element

allowable stress. Hence, it is necessary to develop an improved analytical solution to estimate the span limit. The present study was conducted to determine the reasonable theoretical analysis for the span limit of cable-stayed bridges.

Over the 5,000-year history of engineering structures, bridge spans have been determined mainly by the strength-to-density ratio of available materials. The stiffness and stability of cable-stayed bridges can be improved by changing the cross-sectional form and the spatial distribution of materials or other technical measures (Xiao 2016). The theoretical maximum span length of cable-stayed bridges can be determined based on material strength-to-density ratios (Gimsing and Georgakis 2012, Sun *et al*. 2016). In addition to the theoretical span limit of cable-stayed bridges and its relationship to the strength-to-density ratio of materials, in this study, the span limit of cable-stayed bridges as determined by practical engineering information was defined as the "engineering" span limit. Factors affecting the engineering span limit were analyzed in terms of material strength. Further knowledge regarding the stiffness and stability (e.g., aerodynamic stability) of cable-stayed bridges also merits consideration, but these factors are not discussed in detail here as the focus of this study was only the span limit based on material strength.

2. Theoretical span limit of cable-stayed bridges

2.1 Theoretical span limit determined by the stay cable

The external cable at midspan serves as the research object under the assumption that the external cable projection is one-half of the main span of a super long-span cable-stayed bridge. The equilibrium condition of the infinitesimal cable element with a horizontal projection of dx is shown in Fig. 2.

Equilibrium is defined by $\Sigma X = 0$

$$F_{\mathrm{H}}(x) = F_{\mathrm{H}}(x+\mathrm{d}x) = F_{\mathrm{H}} \tag{1}$$

where $F_{\mathrm{H}}(x)$ is the horizontal component of cable force of the infinitesimal cable element.

Expressing vertical equilibrium from $\Sigma Y = 0$ yields

$$F_{\mathrm{V}}(x) + q\,\mathrm{d}s = F_{\mathrm{V}}(x+\mathrm{d}x) \tag{2}$$

where $F_{\mathrm{V}}(x)$ is the vertical component of cable force of the infinitesimal cable element and q the vertical load intensity along the cable curve.

The equilibrium Eqs. (1) and (2) can be expressed as

$$F_{\mathrm{H}}\frac{\mathrm{d}y}{\mathrm{d}x} + q\sqrt{1+\left(\frac{\mathrm{d}y}{\mathrm{d}x}\right)^2}\,\mathrm{d}x = F_{\mathrm{H}}\frac{\mathrm{d}y}{\mathrm{d}x} + \frac{\mathrm{d}}{\mathrm{d}x}\left(F_{\mathrm{H}}\frac{\mathrm{d}y}{\mathrm{d}x}\right)\mathrm{d}x \tag{3}$$

Eq. (3) is rewritten as

$$\frac{\mathrm{d}\left(\frac{\mathrm{d}y}{\mathrm{d}x}\right)}{\sqrt{1+\left(\frac{\mathrm{d}y}{\mathrm{d}x}\right)^2}} = \frac{q}{F_{\mathrm{H}}}\mathrm{d}x \tag{4}$$

After adding the integral, the result is

$$\frac{\mathrm{d}y}{\mathrm{d}x} = \sinh\left(\frac{q}{F_{\mathrm{H}}}x + C_1\right) \tag{5}$$

Under the theoretical span limit condition, the tangent at the lower end point of the cable is horizontal, in which case the vertical load would induce an infinitely large force in the stay cable (Gimsing and Georgakis 2012); that is, with the coordinate system origin at the lower end of the cable, $y'(0) = 0$; $C_1 = 0$; thus

$$y = \frac{F_{\mathrm{H}}}{q}\cosh\left(\frac{q}{F_{\mathrm{H}}}x\right) + C_2 \tag{6}$$

Introducing $y(0) = 0$ leads to $C_2 = -F_{\mathrm{H}}/q$ so that Eq. (6) can be rewritten as follows

$$y = \frac{F_{\mathrm{H}}}{q}\left[\cosh\left(\frac{q}{F_{\mathrm{H}}}x\right) - 1\right] \tag{7}$$

According to Eq. (5) and $C_1 = 0$, the derivative function follows

$$\frac{\mathrm{d}y}{\mathrm{d}x} = \sinh\frac{q}{F_{\mathrm{H}}}x = \tan\varphi_x \tag{8}$$

where φ_x is the angle between the tangent line of the curve and the ground.

The cable force F_{T} at the upper supporting point with the maximum span length ($x = a_{\max}$) is

$$F_{\mathrm{T}} = F_{\mathrm{H}}\sec\varphi_{x=a_{\max}} = F_{\mathrm{H}}\sqrt{1+(\tan\varphi_{x=a_{\max}})^2} \tag{9}$$

where $a_{\max}$ is the theoretical maximum horizontal projection of the external cable.

Inserting Eq. (8) into Eq. (9) yields the equation

$$F_{\mathrm{T}} = F_{\mathrm{H}}\cosh\left(\frac{q}{F_{\mathrm{H}}}a_{\max}\right) \tag{10}$$

The related conditions are given as

$$\left.\begin{aligned} q &= g_{\mathrm{c}} = \gamma_{\mathrm{c}}A_{\mathrm{c}} \\ F_{\mathrm{T}} &= [\sigma]_{\mathrm{c}}A_{\mathrm{c}} \\ n &= h/(2a_{\max}) = \alpha/2 \\ L_{\mathrm{c,\,max}} &= 2a_{\max} \end{aligned}\right\} \tag{11}$$

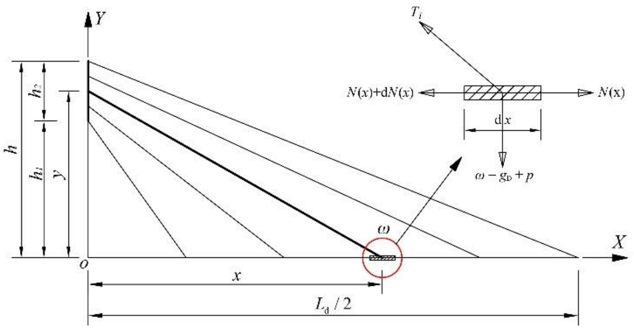

Fig. 3 Horizontal component of the force diagram of cables in a semi-harp system

where g_c denotes the dead load per unit length of the cable, γ_c the weight per unit volume of the cable, A_c the cross-sectional area of the cable, α the inclination of the chord linking the two cable ends, $[\sigma]_c$ the allowable stress of the cable material, n the height-to-span ratio of the cable-stayed bridge, and $L_{c,\max}$ the theoretical maximum span length of the cable-stayed bridge determined by the cable.

Inserting Eq. (11) into Eqs. (7) and (10) yields

$$\left.\begin{aligned} nL_{c,\max} &= \frac{F_H}{g_c}\left[\cosh\left(\frac{g_c}{2F_H}L_{c,\max}\right)-1\right] \\ [\sigma]_c A_c &= F_H\cosh\left(\frac{g_c}{2F_H}L_{c,\max}\right) \end{aligned}\right\} \tag{12}$$

The expression for horizontal force F_H can be derived by rearranging the above equations as follows

$$F_H = (S_c - nL_{c,\max})g_c \tag{13}$$

where $S_c = [\sigma]_c/\gamma_c$ is the strength-to-density ratio of the cable material.

The following equation is derived after substituting Eq. (13) into Eq. (12) and rearrangement

$$\cosh\left(\frac{1}{2}\cdot\frac{L_{c,\max}}{S_c - nL_{c,\max}}\right) = \frac{S_c}{S_c - nL_{c,\max}} \tag{14}$$

where theoretical maximum span length $L_{c,\max}$ is related only to the strength-to-density ratio of the cable material S_c and the height-to-span ratio n.

2.2 Theoretical span limit determined by the girder

There are three main types of cable system: fan, harp, and semi-harp (semi-fan) patterns. The axial compression force on the girder at the pylon of the harp system is twice that of the fan system (Gimsing and Georgakis 2012). Without loss of generality, the semi-harp system is adopted as the research object in this study.

The cable system is shown in Fig. 3. The coordinate system with the origin at the pylon is inconsistent with the equations of theoretical span limit determined by the cable, in which the origin was at the lower cable end.

Under the force of cables, the maximum axial compression force of the girder lays at the intersection with the pylon. The cross-sectional area from midspan to the pylon is expanded by design. Assuming linear and parabolic increases in girder cross-sectional area from the midspan to the pylon, then

$$A_0 = \eta_A A_d^c \tag{15}$$

where η_A denotes the ratio of girder cross-sectional area at the pylon to that of girder at midspan, A_0 the cross-sectional area of the girder at the pylon and A_d^c the cross-sectional area at midspan. $A(x)$ is expressed as

$$A(x) = \begin{cases} \left[\eta_A - (\eta_A - 1)\dfrac{2}{L_d}x\right]A_d^c & \text{for linear increase} \\ \left[1 + (\eta_A - 1)\left(\dfrac{2}{L_d}x - 1\right)^2\right]A_d^c & \text{for parabolic increase} \end{cases} \tag{16}$$

where L_d is the span of the cable-stayed bridge determined by the girder.

Assuming the cable spacing on the girder and pylon are arranged equally and ignoring the adverse effects of cable sag, the horizontal component of the force of a girder segment with a distance x from the pylon under the combination of dead and live loads is

$$\mathrm{d}N(x) = \frac{x}{y}\omega\,\mathrm{d}x = \frac{x}{y}(g_D + p)\,\mathrm{d}x = [\gamma_d A(x) + g_{II} + p]\frac{x}{y}\,\mathrm{d}x \tag{17}$$

where ω denotes the load of the girder per meter of track, g_D the dead load of the girder, γ_d the weight per unit volume of the girder material, and g_{II} the secondary dead load.

k, which denotes the girder-to-pylon ratio of the cable spacing, can be defined as follows

$$k = \frac{\lambda_d}{\lambda_p} = \frac{L_d/2}{h_2} \tag{18}$$

where λ_d denotes the cable spacing of the girder, λ_p the cable spacing of the pylon and h_2 the length of cable-pylon anchorage zone.

The cable equation can be derived as per the geometric relationship in Fig. 3

$$y(x) = h - \left(\frac{L_d}{2} - x\right)\frac{\lambda_p}{\lambda_d} \tag{19}$$

where h is the height of the pylon.

By substituting $A(x)$ and $y(x)$ into Eq. (17) and via integration, the axial pressure of the girder at the pylon N_0 on the assumption of linear and parabolic increases in girder cross-sectional area, respectively, becomes

for linear increase,

$$\begin{aligned} N_0 &= (\gamma_d\eta_A A_d^c + g_{II} + p)k\left[\frac{L_d}{2} + \left(kh - \frac{L_d}{2}\right)\ln\left|\frac{kh - L_d/2}{kh}\right|\right] \\ &+ \frac{2k}{L_d}(\eta_A - 1)\gamma_d A_d^c\left[\left(\frac{khL_d}{2} - \frac{3L_d^2}{8}\right) + \left(kh - \frac{L_d}{2}\right)^2\ln\left|\frac{kh - L_d/2}{kh}\right|\right] \end{aligned} \tag{20}$$

and

for parabolic increase,

$$N_0=(\gamma_{\mathrm{d}}A_{\mathrm{d}}^{\mathrm{c}}+g_{\mathrm{II}}+p)k\left[\frac{L_{\mathrm{d}}}{2}+\left(kh-\frac{L_{\mathrm{d}}}{2}\right)\ln\left|\frac{kh-L_{\mathrm{d}}/2}{kh}\right|\right]+\frac{4k}{L_{\mathrm{d}}^2}(\eta_{\mathrm{A}}-1)\gamma_{\mathrm{d}}A_{\mathrm{d}}^{\mathrm{c}}\left\{\begin{aligned}&\left[\frac{(kh)^2L_{\mathrm{d}}}{2}-\frac{khL_{\mathrm{d}}^2}{8}-\frac{L_{\mathrm{d}}^2}{48}\right]+\\&(kh)^2\left(kh-\frac{L_{\mathrm{d}}}{2}\right)\ln\left|\frac{kh-L_{\mathrm{d}}/2}{kh}\right|\end{aligned}\right\} \tag{21}$$

When axial stress of the girder reaches the material allowable stress, then

$$N_0=[\sigma]_{\mathrm{d}}A_0=[\sigma]_{\mathrm{d}}\eta_{\mathrm{A}}A_{\mathrm{d}}^{\mathrm{c}} \tag{22}$$

where $[\sigma]_{\mathrm{d}}$ denotes the allowable stress of the girder material.

With the height-to-span ratio of the bridge $n=h/L_{\mathrm{d}}$, the strength-to-density ratio of the girder material $S_{\mathrm{d}}=[\sigma]_{\mathrm{d}}/\gamma_{\mathrm{d}}$ and $g_{\mathrm{II}}+p=\gamma_d' A_d^c$, where γ_d' denotes the equivalent additional weight of the girder per unit volume, the following expression for $L_{\mathrm{d,1}}$ assuming linear increase in girder cross-sectional area is derived by combining Eqs. (20) and (22)

$$L_{\mathrm{d,\,l}}=\frac{\eta_{\mathrm{A}}S_{\mathrm{d}}}{k\left\{\left(\eta_{\mathrm{A}}+\frac{\gamma_{\mathrm{d}}'}{\gamma_{\mathrm{d}}}\right)\left[\frac{1}{2}+\left(kn-\frac{1}{2}\right)\ln\left|\frac{kn-1/2}{kn}\right|\right]+2(\eta_{\mathrm{A}}-1)\left[\left(\frac{kn}{2}-\frac{3}{8}\right)+\left(kn-\frac{1}{2}\right)^2\ln\left|\frac{kn-1/2}{kn}\right|\right]\right\}} \tag{23}$$

Similarly, the expression for $L_{\mathrm{d,p}}$ assuming parabolic increase in girder cross-sectional area is derived by combining Eqs. (21) and (22)

$$L_{\mathrm{d,\,p}}=\frac{\eta_{\mathrm{A}}S_{\mathrm{d}}}{k\left\{\left(1+\frac{\gamma_{\mathrm{d}}'}{\gamma_{\mathrm{d}}}\right)\left[\frac{1}{2}+\left(kn-\frac{1}{2}\right)\ln\left|\frac{kn-1/2}{kn}\right|\right]+4(\eta_{\mathrm{A}}-1)\left[\frac{(kn)^2}{2}-\frac{kn}{8}-\frac{1}{48}+(kn)^2\left(kn-\frac{1}{2}\right)\ln\left|\frac{kn-1/2}{kn}\right|\right]\right\}} \tag{24}$$

where when $k\rightarrow\infty$, the cable system is a fan system and L_{d} becomes

$$\left.\begin{aligned}&\text{for linear increase,}\quad \lim_{k\to\infty}L_{\mathrm{d,\,l}}=24n\frac{\eta_{\mathrm{A}}S_{\mathrm{d}}}{\left(\eta_{\mathrm{A}}+3\frac{\gamma_{\mathrm{d}}'}{\gamma_{\mathrm{d}}}+2\right)}\\&\text{for parabolic increase,}\quad \lim_{k\to\infty}L_{\mathrm{d,\,p}}=48n\frac{\eta_{\mathrm{A}}S_{\mathrm{d}}}{\left(\eta_{\mathrm{A}}+6\frac{\gamma_{\mathrm{d}}'}{\gamma_{\mathrm{d}}}+5\right)}\end{aligned}\right\} \tag{25}$$

and when $k\rightarrow L_{\mathrm{d}}/(2h)=1/2n$, the cable system is a harp system and L_{d} becomes

$$\left.\begin{aligned}&\text{for linear increase,}\quad \lim_{k\to1/2n}L_{\mathrm{d,\,l}}=8n\frac{\eta_{\mathrm{A}}S_{\mathrm{d}}}{\left(\eta_{\mathrm{A}}+2\frac{\gamma_{\mathrm{d}}'}{\gamma_{\mathrm{d}}}+1\right)}\\&\text{for parabolic increase,}\quad \lim_{k\to1/2n}L_{\mathrm{d,\,p}}=12n\frac{\eta_{\mathrm{A}}S_{\mathrm{d}}}{\left(\eta_{\mathrm{A}}+3\frac{\gamma_{\mathrm{d}}'}{\gamma_{\mathrm{d}}}+2\right)}\end{aligned}\right\} \tag{26}$$

By comparing Eqs. (25) and (26), when $\eta_{\mathrm{A}}=1$, the span limits $L_{\mathrm{d,1}}$ and $L_{\mathrm{d,p}}$ of cable-stayed bridges with fan systems are twice that of those with harp systems, respectively. This is in accordance with the rule that axial pressure on the girder at the pylon of a harp system is twice that of a fan system.

The expressions derived above are based on the assumption of a continuous distribution of cables and, thus, the results are generalizable. For example, when cables are arranged in a fan shape and the enlargement of the girder cross-sectional area is not considered ($k\rightarrow\infty$, $\eta_{\mathrm{A}}=1$), the axial force distribution of the girder obtained by Eqs. (20) or (21) is consistent with results obtained by Gimsing and Georgakis (2012).

The enlargement ratio of the girder cross-sectional area η_{A} is also an important parameter affecting L_{d}. When $\eta_{\mathrm{A}}\rightarrow\infty$, Eqs. (23) and (24) becomes

$$\left.\begin{aligned}&\text{for linear increase,}\\&\lim_{\eta_{\mathrm{A}}\to\infty}L_{\mathrm{d,\,l}}=\frac{S_{\mathrm{d}}}{k\left\{\left[\frac{1}{2}+\left(kn-\frac{1}{2}\right)\ln\left|\frac{kn-1/2}{kn}\right|\right]+2\left[\left(\frac{kn}{2}-\frac{3}{8}\right)+\left(kn-\frac{1}{2}\right)^2\ln\left|\frac{kn-1/2}{kn}\right|\right]\right\}}\\&\text{for parabolic increase,}\\&\lim_{\eta_{\mathrm{A}}\to\infty}L_{\mathrm{d,\,p}}=\frac{S_{\mathrm{d}}}{4k\left\{\left[\frac{(kn)^2}{2}-\frac{kn}{8}-\frac{1}{48}\right]+(kn)^2\left(kn-\frac{1}{2}\right)\ln\left|\frac{kn-1/2}{kn}\right|\right\}}\end{aligned}\right\} \tag{27}$$

Clearly, the span limit of the cable-stayed bridge determined by the girder increases as k and η_{A} increase, thus, when $k\rightarrow\infty$ and $\eta_{\mathrm{A}}\rightarrow\infty$, the theoretical maximum span length determined by the girder assuming linear and parabolic increases in girder cross-sectional area, respectively, becomes

$$\text{for linear increase,}\quad L_{\mathrm{d,\,max}}=\lim_{\eta_{\mathrm{A}}\to\infty}(\lim_{k\to\infty}L_{\mathrm{d,\,l}})=24n\cdot S_{\mathrm{d}} \tag{28}$$

and

$$\text{for parabolic increase,}\quad L_{\mathrm{d,\,max}}=\lim_{\eta_{\mathrm{A}}\to\infty}(\lim_{k\to\infty}L_{\mathrm{d,\,p}})=48n\cdot S_{\mathrm{d}} \tag{29}$$

where $L_{\mathrm{d,max}}$ denotes the theoretical maximum span length of the cable-stayed bridge determined by the girder.

The above derivation also suggests that the theoretical span limit determined by the girder is also related only to the strength-to-density ratio of the girder material and the height-to-span ratio of the bridge. The theoretical maximum span length of cable-stayed bridges with a parabolic increase assumption is twice that under a linear increase assumption.

The cable inclination angle is less than that of the pylon such that the horizontal component force of the girder is much greater than that of the vertical component force of the pylon. As a result, the theoretical span limit is determined by the girder. The span limit determined by the pylon is not specifically discussed here for this reason.

2.3 Theoretical span limit of cable-stayed bridges

The solutions for $L_{\mathrm{c,max}}$ and $L_{\mathrm{d,max}}$ are obtained once the strength-to-density ratio of the cable material S_{c}, strength-to-density ratio of the girder material S_{d}, and height-to-span ratio n of the cable-stayed bridge are determined. The theoretical maximum span length of the cable-stayed bridge is the smaller of the two values:

$$L_{\max}=\min\{L_{\mathrm{c,\,max}},L_{\mathrm{d,\,max}}\} \tag{30}$$

where $L_{\mathrm{c,max}}$ denotes the theoretical maximum span length determined by the cable and $L_{\mathrm{d,max}}$ the theoretical

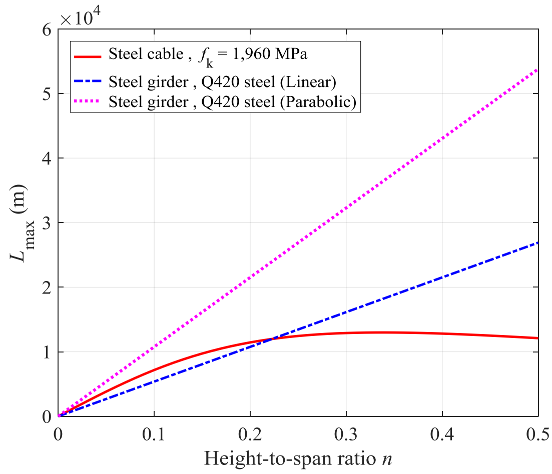

Fig. 4 Relationship between theoretical span limit and height-to-span ratio

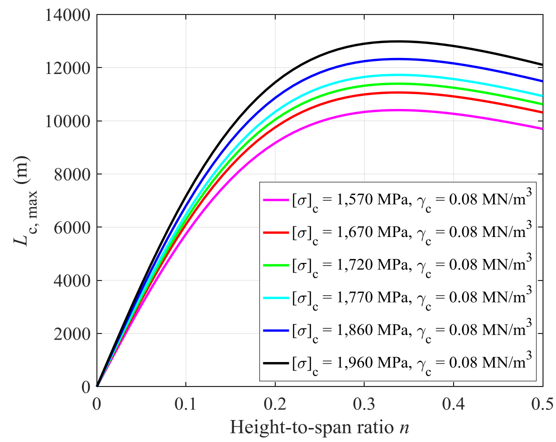

Fig. 5 Relationship between span limit and height-to-span ratio with varying cable strengths

maximum span length determined by the girder. According to relevant parameters from existing actual long-span cable-stayed bridge projects, the theoretical span limit is determined by the strength-to-density ratio of the cable and girder, respectively.

For super long-span bridges, steel is still the most commonly used construction material. Other materials such as fiber-reinforced polymer (FRP) and composites (Xiong *et al*. 2011, Hassan *et al*. 2014, Kirkland and Uy 2015), even though available currently, are not yet ready for extensive use in the construction of long-span bridges. For this reason, the steel cable-stayed bridge only is considered in the following analysis.

The theoretical span limits determined by cable and girder with different height-to-span ratios under the following parameters are shown in Fig. 4: $[\sigma]_c$ = 784 MPa (f_k = 1,960 MPa), $\gamma_c = 8\times10^4$ N/m^3 (including corrosion protection), $[\sigma]_d$ = 220 MPa (Q420qD steel, with yield stress 420 MPa), and $\gamma_d = 7.85\times10^4$ N/m^3, respectively.

When the height-to-span ratio (n < 0.1) is relatively small, the theoretical span limit determined by the cable is almost proportional to the height-to-span ratio. When n is larger, the increase in the theoretical span length slows down as the curve progresses; the theoretical span limit starts to curve downwards and a maximum is reached for n = 0.34, where $L_{c,max}$ = 12,989 m, and then the curve gradually declines. The maximum height-to-span ratio 0.34 exceeds the 0.18-0.26 range used in existing cable-stayed bridges. For the typical height-to-span ratio, n = 0.2, the theoretical span limit of cable-stayed bridges determined by the cable is 11,450 m. The theoretical span limit determined by the girder increases linearly with the height-to-span ratio. When the height-to-span ratio is below 0.22, the theoretical span limit of the cable is greater than that of the girder assuming a linear increase in girder cross-sectional area. After that point, the theoretical span limit of the girder (assuming a linear increase in girder cross-sectional area) exceeds that of the cables as the height-to-span ratio further increases. The theoretical span limit of the girder, assuming a parabolic increase in girder cross-sectional area, is always greater than that of the cable. In this case, the theoretical span limit of the cable-stayed bridge is determined by the cable.

In addition to the height-to-span ratio n, the strength-to-density ratio of materials (S_c, S_d) is an important parameter determining the theoretical span limit. The theoretical span limit of the girder has an explicit linear relationship with the strength-to-density ratio of the girder. The relationship between the theoretical span limit and height-to-span ratio with varying cable strengths is shown in Fig. 5. In addition to the girder, there is a proportional relationship between the theoretical span limit and strength-to-density ratio of the cable.

3. Engineering span limit of cable-stayed bridges

The theoretical span limit of the cable assumes that external cable force is infinite, which does not represent the actual ability to provide vertical support. The theoretical span limit of the girder assumes that all cables are anchored to the top of the pylon and that the maximum cross-sectional area of the girder tends towards infinity. Clearly, these assumptions do not apply to actual projects. To ensure a rational estimation of the span limit of cable-stayed bridges, it is necessary to establish the "engineering" span limit.

3.1 Engineering span limit determined by the stay cable

The differential equation (Eq. (4)) of the microelement equilibrium after two integrations and rearrangement is

$$y = \frac{F_H}{g_c}\cosh\left(\frac{g_c}{F_H}x + C_1\right) + C_2 \tag{31}$$

Introducing the boundary condition $y(0) = 0$ leads to $C_2 = -\frac{F_H}{g_c}\cosh C_1$, and C_1 can be rewritten as C to derive the general equation of the cable geometry

$$y = \frac{F_H}{g_c}\left[\cosh\left(\frac{g_c}{F_H}x + C\right) - \cosh C\right] \tag{32}$$

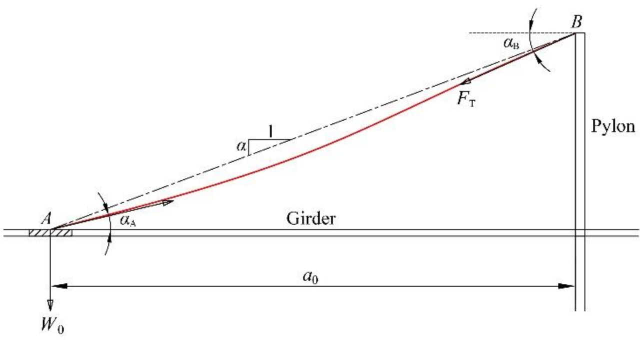

Fig. 6 Force diagram of external cable with span limit

The derivative function at the anchorage point of the girder and pylon are, respectively, written as

$$\left.\begin{aligned} y'(0) &= \tan\varphi_{x=0} = \sinh C = \tan\alpha_A \\ y'(a_0) &= \tan\varphi_{x=a_0} = \sinh\left(\frac{g_c}{F_H}a_0 + C\right) = \tan\alpha_B \end{aligned}\right\} \tag{33}$$

where a_0 is the horizontal projection length of the external cable.

At the anchorage point of the girder, it is assumed that the external cable supports dead and live loads on the girder segment within the cable spacing as well as half of the self-weight of the cable (Fig. 6)

$$W_0 = W_D + W_L + W_c/2 \tag{34}$$

with the following equations

$$\left.\begin{aligned} W_D &= g_D\lambda \\ W_L &= p\lambda \\ W_c &= g_c s_0 \end{aligned}\right\} \tag{35}$$

where W_0 denotes the total cable tributary weight of the girder within the cable spacing; W_D, W_L, W_c denote the dead load, live load, and cable self-weight within the cable spacing, respectively. s_0 is the non-stress length of external cable, which is determined as follows

$$s_0 = s - \Delta s = \int_0^{a_0}\sqrt{1+\left(\frac{dy}{dx}\right)^2}\,dx - \frac{F_H}{E_c A_c}\int_0^{a_0}\left[1+\left(\frac{dy}{dx}\right)^2\right]dx \tag{36}$$

where E_c denotes the elastic modulus of the cable.

The expression for s_0 is derived after integration and rearrangement as

$$\begin{aligned} s_0 = {} & \frac{F_H}{g_c}\left[\sinh\left(\frac{g_c}{F_H}a_0 + C\right) - \sinh C\right] \\ & - \frac{F_H}{2E_c A_c}\left\{a_0 + \frac{F_H}{2g_c}\left\{\sinh\left[2\left(\frac{g_c}{F_H}a_0 + C\right)\right] - \sinh 2C\right\}\right\} \end{aligned} \tag{37}$$

Expressing vertical equilibrium at the anchorage point of the girder yields

$$\sum F_y = 0 \quad W_0 = F_H \tan\alpha_A \tag{38}$$

Combining Eqs. (34)-(38) and rearranging them with $W_\lambda = (g_D + p)\,\lambda$ yields

$$\begin{aligned} & 2W_\lambda + F_H\left[\sinh\left(\frac{g_c}{F_H}a_0 + C\right) - 3\sinh C\right] \\ & = \frac{g_c F_H}{2E_c A_c}\left\{a_0 + \frac{F_H}{2g_c}\left\{\sinh\left[2\left(\frac{g_c}{F_H}a_0 + C\right)\right] - \sinh 2C\right\}\right\} \end{aligned} \tag{39}$$

where W_λ denotes the load weight on the girder within the cable spacing.

The cable force at the upper supporting point F_T is

$$F_T = F_H \sec\varphi_{x=a_0} = F_H\sqrt{1+(\tan\varphi_{x=a_0})^2} \tag{40}$$

Inserting Eq. (33) into Eq. (40) yields

$$F_T = F_H \cosh\left(\frac{g_c}{F_H}a_0 + C\right) \tag{41}$$

Upon reaching the span limit state, the cable conditions are

$$\left.\begin{aligned} y(a_0) &= h = \alpha a_0 = nL_c \\ F_T &= [\sigma]_c A_c \end{aligned}\right\} \tag{42}$$

where L_c is the span length of the cable-stayed bridge determined by the cable.

Inserting into Eqs. (32) and (41) yields

$$\left.\begin{aligned} nL_c &= \frac{F_H}{g_c}\left[\cosh\left(\frac{g_c}{2F_H}L_c + C\right) - \cosh C\right] \\ [\sigma]_c A_c &= F_H \cosh\left(\frac{g_c}{2F_H}L_c + C\right) \end{aligned}\right\} \tag{43}$$

The following expression for horizontal force F_H can be derived by rearrangement of the above equations

$$F_H = \frac{1}{\cosh C}\cdot(S_c - nL_c)g_c \tag{44}$$

By comparison with Eq. (13), the horizontal force of the cable under the engineering span limit state determined by the cable is smaller than that under the theoretical span limit state. The ratio of the two is $1/\cosh C$.

Substituting Eq. (44) into Eq. (43) yields

$$\cosh\left(\frac{1}{2}\cdot\frac{L_c}{S_c - nL_c} + C\right) = \cosh C\cdot\frac{S_c}{S_c - nL_c} \tag{45}$$

By comparison with Eq. (14), the engineering span limit and horizontal component force of the cable are not only determined by the strength-to-density ratio of the cable material and the height-to-span ratio of the bridge, but are also related to the constant C. Equation (39) indicates that the constant C is also related to the load weight within the cable spacing and the cable self-weight.

The following equations can be written by combining Eqs. (39) and (43)

$$\left.\begin{aligned} nL_{\mathrm{c}} &= \frac{F_{\mathrm{H}}}{g_{\mathrm{c}}}\left[\cosh\left(\frac{g_{\mathrm{c}}}{2F_{\mathrm{H}}}L_{\mathrm{c}}+C\right)-\cosh C\right] \\ [\sigma]_{\mathrm{c}}A_{\mathrm{c}} &= F_{\mathrm{H}}\cosh\left(\frac{g_{\mathrm{c}}}{2F_{\mathrm{H}}}L_{\mathrm{c}}+C\right) \\ 2W_{\lambda}+F_{\mathrm{H}}\left[\sinh\left(\frac{g_{\mathrm{c}}}{2F_{\mathrm{H}}}L_{\mathrm{c}}+C\right)-3\sinh C\right] &= \frac{g_{\mathrm{c}}F_{\mathrm{H}}}{4E_{\mathrm{c}}A_{\mathrm{c}}}\left\{L_{\mathrm{c}}+\frac{F_{\mathrm{H}}}{g_{\mathrm{c}}}\left\{\sinh\left[\left(\frac{g_{\mathrm{c}}}{F_{\mathrm{H}}}L_{\mathrm{c}}+2C\right)\right]-\sinh 2C\right\}\right\} \end{aligned}\right\} \quad (46)$$

The above system of nonlinear equations contains three unknown parameters (F_{H}, L_{c}, and C) and three equations. When the parameters $[\sigma]_{\mathrm{c}}$, γ_{c}, E_{c}, A_{c}, and n are all known, the engineering limit span length of the cable-stayed bridge determined by the cable L_{c} and horizontal force F_{H} of the cable and the constant C can be accurately determined. The specific equation of the external cable curve can be determined accordingly.

3.2 Engineering span limit determined by the girder

The engineering span limit of the girder is determined by the general formulas Eqs. (23) and (24) as derived in the previous section. When parameters η_{A}, S_{d}, γ'_{d}, k, and n are all known, the engineering span limit of the cable-stayed bridge determined by the girder is obtained.

It is worth mentioning here that the bending moment effect of dead and live loads on the girder is not included in the above derivations. For super long-span cable-stayed bridges, the stress due to bending is not significant and the effect considered by reducing the value of allowable girder stress. It is assumed that the allowable girder stress $[\sigma]_{\mathrm{d}}$ is reduced by 20% after considering the bending moment (Tang 2017); that is, the allowable stress $[\sigma]_{\mathrm{d}}$ multiplied by a correction coefficient 0.8 is substituted into the above equations for analysis. Assuming the girder adopted is Q420qD steel, for example, the allowable stress is $[\sigma]_{\mathrm{d}}$ = 176 MPa.

3.3 Engineering span limit of cable-stayed bridges

When the material and design parameters are given, the engineering span limit of the cable-stayed bridge L can be expressed as

$$L = \min\{L_{\mathrm{c}}, L_{\mathrm{d}}\} \quad (47)$$

where L_{c} denotes the engineering span limit determined by the cable and L_{d} the engineering span limit determined by the girder. The engineering span limit of the cable-stayed bridge L is the smaller value of the two.

4. Engineering span limit parametric analysis

For the purposes of parametric analysis, the design parameters of materials and the structural system of cable-stayed bridges are kept within a reasonable range in terms of actual engineering applications. In addition to the material parameters of the cable and girder discussed in the above theoretical span limit analysis, in actual engineering scenarios, the height-to-span ratio of cable-stayed bridges is generally 0.18-0.26. The cable spacing λ is generally 10-20 m. The maximum cross-sectional area of a single cable is 0.018 m^2 for double cable planes and thus A_{c} = 0.036 m^2. The enlargement ratio of the girder cross-sectional area η_{A} is usually around 1.25. The girder-to-pylon ratio of the cable spacing k is typically 5. The dead load intensity of the Sutong Bridge is 2.02×10^5 N/m and that of Stonecutters Bridge 2.62×10^5 N/m. Considering the maximum span range discussed here, the values of g_{D} selected are (2-4) ×10^5 N/m (including the secondary dead load, where g_{II} = 7×10^4 N/m). Live loads in design codes of most countries are composed of a uniformly distributed load and several concentrated loads. In super long-span bridges, especially in the preliminary design stage, concentrated loads can be safely represented as a uniformly distributed load with an amplification factor (Sun *et al.* 2016). Thus, live load intensity p, considering the multi-function traffic of long-span cable-stayed bridges with eight traffic lanes and concentrated live load (for heavy trucks) with an amplification factor 1.5 (Zhang 2013), can be safely set to 7×10^4 N/m. The engineering span limit and parametric analysis of cable-stayed bridges are discussed below based on these basic design parameters.

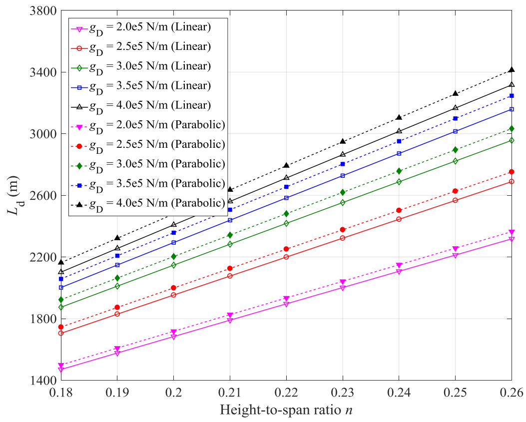

Fig. 7 Relationship between engineering span limit of the girder and height-to-span ratio (λ = 15 m)

4.1 Relationship between height-to-span ratio and engineering span limit

According to Eqs. (23) And (24), different load weights affect the relationship between the engineering span limit L_{d} and height-to-span ratio n (0.18-0.26) as such that the

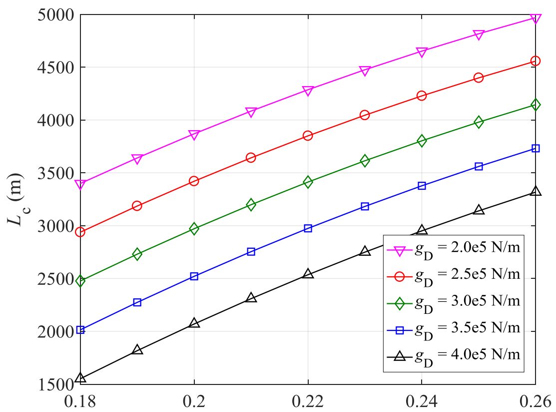

(a) Variations in load weight (λ = 15 m)

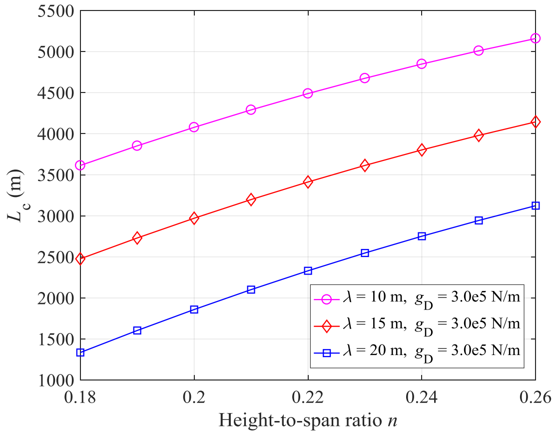

(b) Variations in cable spacing (g_D = 30 t/m)

Fig. 8 Relationship between engineering span limit of load-carrying cable and height-to-span ratio

engineering span limit L_d increases linearly as height-to-span ratio increases (Fig. 7). Under the same height-to-span ratio, the engineering span limit L_d increases as load weight increases. This is mainly because load weight is closely related to girder cross-sectional area and, accordingly, the limit span length increases with the cross-section. The increase in engineering span limit L_d also slows down as the load weight increases.

The engineering span limit of the girder under a parabolic increase assumption is greater than that under a linear increase assumption, which is illustrated above as dotted lines of uniform color above solid lines. When the load weight on the girder is 5.55 MN ($g_D = 3\times10^5$ N/m, $p = 7\times10^4$ N/m, and λ = 15 m) and the height-to-span ratio is 0.2, the span limit of the cable-stayed bridge determined by the girder under linear and parabolic increases in girder cross-sectional area are 2,147.3 m and 2,203.2 m, respectively. When the height-to-span ratio is increased to 0.22, the engineering span limit L_d increases to 2,418.4 m and 2,481.2 m, respectively. Unlike the theoretical span limit discussed above, when design parameters are within the scope of actual engineering applications, there is not much difference between the engineering span limit of the girder with parabolic and linear increase assumptions.

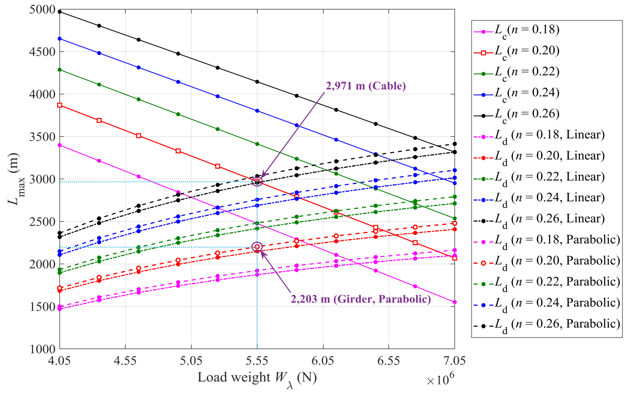

Fig. 9 Relationship between engineering span limit and load weight

According to Eq. (46), when different load weights are used, the relationship between the engineering span limit L_c and height-to-span ratio n (0.18-0.26) results in a nonlinear increase in engineering span limit L_c with height-to-span ratio n as shown in Fig. 8.

When the load weight on the girder is 5.55 MN ($g_D = 3\times10^5$ N/m) and the height-to-span ratio 0.2, the span limit of the cable-stayed bridge determined by the cable is2,970.9 m. When the height-to-span ratio is 0.22, the engineering span limit L_c increases to 3,412.6 m.

Contrary to the trend of the engineering span limit being determined by the girder, the engineering span limit L_c decreases linearly as load weight increases when the height-to-span ratio remains constant. (The effect of load weight on the span limit of the bridge is discussed in greater detail below.) The engineering span limit of load-carrying cables increases as the cable spacing on the girder decreases (Fig. 8b). When the load weight on the girder is 5.55 MN ($g_D = 3\times10^5$ N/m), cable spacing 10 m and height-to-span ratio 0.2, the span limit of the bridge determined by the load-carrying cable is 4,078.1 m. When the cable spacing is increased to 20 m, the engineering span limit is reduced to 1,859.2 m.

4.2 Relationship between load weight and engineering span limit

Relationship curves of the span limit with load weight under different height-to-span ratios (Eqs. (23)-(24) and (46)) show that the engineering span limit of load-carrying cable decreases as load weight increases and the span of the girder increases with load weight (Fig. 9). When the load weight is small, the engineering span limit of the bridge is determined by the girder (solid lines of uniform color above dotted and dot-dash lines). As load weight increases, the engineering span limit of load-carrying cable decreases while that of the girder increases and the two span lengths approach each other (solid lines of uniform color intersecting dotted and dot-dash lines). At this point, the material performance of both the cable and girder are fully utilized. With further increases in load weight, the engineering span limit determined by the girder starts to exceed that of load-carrying cable (dotted and dot-dash

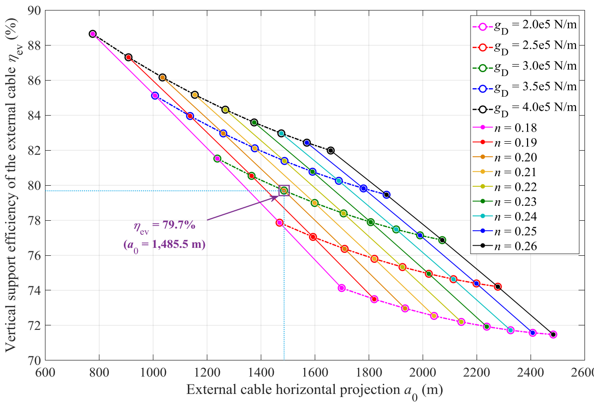

Fig. 10 Relationship between vertical support efficiency and external cable horizontal projection

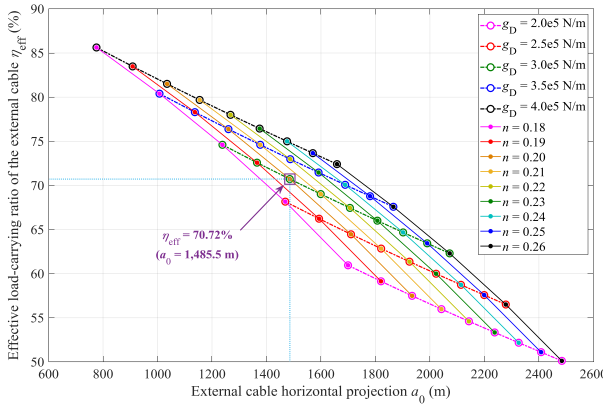

Fig. 11 Relationship between effective load-carrying ratio and external cable horizontal projection

lines of uniform color above solid lines).

Under the height-to-span ratio of 0.2 and girder load weight of 5.55 MN ($g_D = 3\times10^5$ N/m), the engineering limit length of the bridge determined by the cable is 2,970.9 m and that determined by the girder is 2,203.2 m (parabolic assumption). The girder is dominant under this condition, which is common in engineering practice. When the load weight on the girder is increased to 7.05 MN ($g_D = 4\times10^5$ N/m, $p = 7\times10^4$ N/m, and $\lambda = 15$ m), the span limit of the bridge determined by the cable decreases to 2,069.8 m while that determined by the girder increases to 2,408.4 m (linear assumption). In this case, the engineering span limit of the bridge is determined by the cable.

In practical engineering, the cable spacing can be reduced (and load weight reduced accordingly) and the cable diameter can also be reasonably increased. Unlike the theoretical engineering span limit, the critical member which determines the engineering span limit is the girder with respect to allowable stresses (based on the materials available today). The engineering span limit of cable-stayed bridges with respect to allowable stresses is around 2,200 m as determined by the girder under the typical values of height-to-span ratio $n = 0.2$ and load weight $W_\lambda = 5.55$ MN ($g_D = 3\times10^5$ N/m) as shown in Fig. 9

4.3 Vertical support efficiency of stay cables

As the sag of cables is proportional to the length of the chord, the effects of cable sag are highly pronounced in long-span bridges. The cable angle at the girder anchorage point is reduced when span is long, which significantly reduces the vertical support efficiency. The vertical support efficiency of the sagging cable η_{ev} is defined to express the extent to which load-carrying capacity is reduced due to cable sag

$$\eta_{ev} = \frac{F_{Vc}}{F_{V0}} = \frac{\sin\alpha_A}{\sin\alpha_0} \tag{48}$$

where F_{vc} and F_{v0} denote the vertical force component of the cable with sag or without, respectively; α_A is the cable angle at the girder anchorage point and α_0 the angle of the chord of the inclined cable.

The vertical support efficiency and horizontal projection of cables are plotted under different height-to-span ratios and load weights (Eqs. (46) and (48)) as shown in Fig. 10. The solid line represents the relationship between the vertical support efficiency and horizontal projection of the cable at the same height-to-span ratio but different load weights and the dotted line represents the relationship between the vertical support efficiency and horizontal projection of the cable at the same load weight but different height-to-span ratios.

The vertical support efficiency of the cable decreases as the horizontal projection length increases. When the horizontal projection of the cable is constant, the vertical support efficiency of the cable increases with load weight and height-to-span ratio and is mainly affected by load weight.

When the girder load weight is 5.55 MN ($g_D = 3\times10^5$ N/m) and the height-to-span ratio is 0.2, the inclination angle of the external cable at the girder anchorage point α_A can be obtained according to Eq. (33) where α_A = arctan(sinh$C$) = 17.22°; this value is considerably smaller than the chordal inclination of the cable curve α_0 = arctan(2n) = 21.80°. The cable end angle decreases as cable length increases due to cable sag, which weakens the support efficiency. If the vertical support efficiency of cables for cable-stayed bridges is required to be at least 80%, according to Eq. (48), the vertical support efficiency of the cable will be η_{ev} = 79.7%, which is slightly less than 80%; the horizontal projection length is 1,485.5 m ($g_D = 3\times10^5$ N/m, $n = 0.2$). When the girder load weight is 7.05 MN ($g_D = 4\times10^5$ N/m) and the height-to-span ratio is 0.24, the horizontal projection length is 1,476 m, which is close to 1,485.5 m, and the vertical support efficiency of the external cable is 83%. When the girder load weight is 4.05 MN ($g_D = 2\times10^5$ N/m, $p = 7\times10^4$ N/m, and $\lambda = 15$ m) and the height-to-span ratio is 0.25, the vertical support efficiency of the horizontal projection length of 2,408 m of the external cable is only 71.6%.

4.4 Effective load-carrying ratio of stay cables

As the length of the stay cable increases, its self-weight synchronously increases and the proportion of cable tension used to carry its own weight increases as well. The effective carrying capacity of stay cables η_{eff} is defined as

$$\eta_{\mathrm{eff}} = \frac{W_{\mathrm{D}} + W_{\mathrm{L}}}{W_0} \tag{49}$$

This expression represents the proportion of the external load (girder, secondary dead load, and live load) carried by the stay cable in the total cable force.

The relationship between effective load-carrying ratio and cable horizontal projection under different height-to-span ratios and load weights (Eqs. (46) and (49)) is shown in Fig. 11. The solid line marks the relationship between effective load-carrying ratio and cable horizontal projection at the same height-to-span ratio but different load weights and the dotted line shows the relationship between effective load-carrying ratio and cable horizontal projection at the same load weight but different height-to-span ratios. Similar to the law of cable vertical support efficiency, the effective load-carrying ratio of the cable decreases as horizontal projection length increases. When the horizontal cable projection is constant, the effective load-carrying ratio of the cable increases with load weight and height-to-span ratio, which is mainly affected by load weight.

When the load weight on the girder is 5.55 MN ($g_{\mathrm{D}} = 3\times10^5$ N/m) and the height-to-span ratio is 0.2, the effective load-carrying ratio with a 1,485.5 m external cable horizontal projection length is 70.72%; that is, the proportion of cable tension used to carry its own weight is about 29.3%. When the girder load weight is 7.05 MN ($g_{\mathrm{D}} = 4\times10^5$ N/m) and the height-to-span ratio is 0.24, the horizontal projection length is 1,475.6 m (i.e., close to 1,485.5 m) and the effective load-carrying ratio of external cable increases to 75%. When the girder load weight is 4.05 MN ($g_{\mathrm{D}} = 2\times10^5$ N/m) and the height-to-span ratio is 0.25, the effective load-carrying ratio with a 2,408 m horizontal projection length for the external cable is only 51.1%; that is, upon reaching the engineering span limit, the weight of the cable comprises nearly 50% of the cable force.

5. Conclusions

The results of this study can be summarized as follows:

• Cable-stayed bridges have theoretical span limits that can be determined only by the strength-to-density ratio and height-to-span ratio. However, the assumptions of the theoretical span limit for cable-stayed bridges do not apply to actual projects. The engineering span limit must be rationally used to estimate the span limit of cable-stayed bridges.

• The engineering span limit of a cable-stayed bridge is not only related to its height-to-span ratio and strength-to-density ratio of its material but also to the actual loading conditions and structural design (e.g., dead and live loads on the girder and the cross-sectional area of the cable and girder).

• Approaches to increasing the engineering span limit include increasing the strength-to-density ratio of the cable and girder materials of the bridge, decreasing the cable spacing on the girder, and increasing the height-to-span ratio appropriately.

• Current technological, economic, and functional indices allow for cable-stayed bridges with an engineering span limit of about 2,200 m based on the allowable steel stress. (That is, assuming the girder adopted is Q420qD steel and the typical values of height-to-span ratio n = 0.2 and load weight W_λ = 5.55 MN ($g_{\mathrm{D}} = 3\times10^5$ N/m, λ = 15 m). The girder is the critical member which determines the span limit owing to the substantial axial pressure caused by stay cables.

• The stiffness and stability (including aerodynamic stability) of cable-stayed bridges which are also key factors in determining the span limit must be technically resolved to ensure that the span lengths approach the engineering span limit.

Acknowledgments

The authors gratefully acknowledge the financial support provided by the Science and Technology Committee of Shanghai, China (Grant No. 17DZ1204204 and Grant No. 16ZR1439000). The opinions and statements expressed in this paper do not necessarily represent those of the sponsors.

References

Cao, J., Ge, Y. and Yang, Y. (2009), "Structural static performance of cable-stayed bridges with super long spans", *Computational Structural Engineering: Proceedings of the International Symposium on Computational Structural Engineering*, Shanghai, June.

Hassan, M.M., Damatty, E.A, and Nassef, A.O. (2014), "Database for the optimum design of semi-fan composite cable-stayed bridges based on genetic algorithms", *Struct. Infrastruct. Eng.*, **11**(8), 1054-1068. https://doi.org/10.1080/15732479.2014.931976.

Gimsing, N.J. (2005), "The modern cable-stayed bridge - 50 years of development from 1955 to 2005", *Proceedings of the International Symposium on Innovation and Sustainability of Structures in Civil Engineering*, Nanjing, November.

Gimsing, N.J. and Georgakis, C.T. (2012), *Cable Supported Bridges: Concept and Design*, (3rd Edition), John Wiley and Sons, Ltd., Chichester, United Kingdom.

Kirkland, B. and Uy, B. (2015), "Behaviour and design of composite beams subjected to flexure and axial load", *Steel Compos. Struct.*, **19**(3), 615-633. https://doi.org/10.12989/scs.2015.19.3.615.

Leonhardt, F., and Zeller, W. (1991), "Past, present and future of cable-stayed bridges", *Cable-stayed bridges—Recent developments and their future: Proceedings of the Seminar*, Yokohama, December.

Lewis, W.J. (2012), "A mathematical model for assessment of material requirements for cable supported bridges: implications for conceptual design", *Eng. Struct.*, **42**(9), 266-277. https://doi.org/10.1016/j.engstruct.2012.04.018.

Nagai, M., Fujino, Y., Yamaguchi, H., and Iwasaki, E. (2004), "Feasibility of a 1,400 m span steel cable-stayed bridge", *J. Bridge Eng.*, **9**(5), 444-452. https://doi.org/10.1061/(ASCE)1084-0702(2004)9:5(444).

Sun, B., Zhang, L.W., Qin, Y.D., and Xiao, R.C. (2016), "Economic performance of cable supported bridges", *Struct. Eng. Mech.*, **59**(4), 621-652. https://doi.org/10.12989/sem.2016.59.4.621.

Tang, M.C. (2014), "Concept of a bridge across the Taiwan Strait", *Proceedings of the 10th Conference on Bridge and Tunnel*

Connection across the Taiwan Strait, Fuzhou, November.
Tang, M.C. (2017), "Super-long span bridges", *Struct. Infrastruct. Eng.*, **13**(6), 722-730. https://doi.org/10.1080/15732479.2016.1187635.
Virlogeux, M. (1999), "Recent evolution of cable-stayed bridges", *Eng. Struct.*, **21**(8), 737-755. https://doi.org/10.1016/S0141-0296(98)00028-5.
Wang, B.H. (2002), "Extreme span length of cable-stayed bridge", *Highway*, **3**(3), 38-48.
Wu, X.G. (1996), "Analysis on limit span of cable-stayed bridges", *J. Chongqing Jiaotong Institute*, **15**(3), 36-38.
Xiao, R.C. (2016), *Bridge Structural Systems*, S.K. Kataria and Sons, New Delhi, India.
Xiong, W., Cai, C.S., Zhang, Y., and Xiao, R.C. (2011). "Study of super long span cable-stayed bridges with CFRP components", *Eng. Struct.*, **33**(2), 330-343. https://doi.org/10.1016/j.engstruct.2010.10.013.
Zhang, Y.Y. (2013), "Limitation span of self-anchored cable-stayed bridge", *J. Chongqing Jiaotong U*, **32**(2), 177-182.

PL

Notation

The following symbols are used in this paper:

A_0 = cross-sectional area of the girder at the pylon;

A_c = cross-sectional area of the cable;

A_d^c = cross-sectional area of the girder at midspan;

E_c = elastic modulus of the cable;

F_H = horizontal component of cable force;

F_T = cable force at the upper supporting point;

F_V = vertical component of cable force;

F_{V0} = vertical force component of the cable without sag;

F_{Vc} = vertical force component of sagging cable;

L = engineering span limit of the cable-stayed bridge;

L_c = engineering span limit determined by the cable;

$L_{c,\max}$ = theoretical maximum span length of the cable-stayed bridge determined by the cable;

L_d = engineering span limit determined by the girder;

$L_{d,1}$ = span limit of the cable-stayed bridge assuming linear increase in girder cross-sectional area;

$L_{d,\max}$ = theoretical maximum span length of the cable-stayed bridge determined by the girder;

$L_{d,p}$ = span limit of the cable-stayed bridge assuming parabolic increase in girder cross-sectional area;

$L_{\max}$ = theoretical maximum span length of the cable-stayed bridge;

N_0 = axial pressure of the girder at the pylon;

S_c = strength-to-density ratio of the cable material;

S_d = strength-to-density ratio of the girder material;

W_0 = total cable tributary weight of the girder within the cable spacing;

W_D = dead load within the cable spacing;

W_L = live load within the cable spacing;

W_c = cable self-weight within the cable spacing;

W_λ = load weight on the girder within the cable spacing;

a_0 = horizontal projection length of the external cable;

$a_{\max}$ = theoretical maximum horizontal projection of the external cable;

g_D = dead load of the girder;

g_c = dead load per unit length of the cable;

g_{II} = secondary dead load;

h = height of the pylon;

h_2 = length of cable-pylon anchorage zone;

k = girder-to-pylon ratio of the cable spacing;

n = height-to-span ratio of the cable-stayed bridge;

p = live load intensity on the girder;

q = vertical load intensity along the cable curve;

s_0 = non-stress length of external cable;

α = inclination of the chord linking the two cable ends;

α_0 = angle of the chord of the inclined cable;

α_{A} = cable angle at the girder anchorage point;

α_{B} = cable angle at the pylon anchorage point;

$[\sigma]_{\mathrm{c}}$ = allowable stress of the cable;

$[\sigma]_{\mathrm{d}}$ = allowable stress of the girder;

η_{A} = ratio of girder cross-sectional area at the pylon to that of girder at midspan;

η_{eff} = effective carrying capacity of stay cables;

η_{ev} = vertical support efficiency of sagging cable;

γ_{c} = weight per unit volume of the cable;

γ_{d} = weight per unit volume of the girder;

γ'_{d} = equivalent additional weight of the girder per unit volume;

λ_{d} = cable spacing of the girder;

λ_{p} = cable spacing of the pylon;

ω = load of the girder per meter of track; and

φ_x = angle between the tangent line of the curve and the ground